HFPC´89 Conference, Naples, May 15-18, 1989

ANALYSIS OF THE CASCADE-CONTROL BEHAVIOR OF A BIDIRECTIONAL HIGH-FREQUENCY DC-DC-CONVERTER

Felix A. HIMMELSTOSS, Johann W. KOLAR and Franz C. ZACH

Technical University of Vienna - Power Electronics Section
Gusshausstrasse 27-29, A - 1040 Vienna, AUSTRIA

A B S T R A C T

A system for DC-DC power conversion based on a buck-boost converter topology is presented which makes power flow in both directions possible. The possibility of bidirectional power flow is useful for certain applications, such as uninterruptable power supplies (UPS) etc. Starting from a structure diagram the transfer function of the system is split up. The controller for the converter is then realized as voltage controller with an inner loop current controller. The transfer functions of the different system parts are derived and dimensioning guidelines for the controller sections are presented. The closed loop control is treated based on simulation using duty cycle averaging. The closed-loop behavior of the bidirectional converter with cascade control is analyzed; bode-diagrams are shown for the system sections and for the overall system. The design of a controller is shown for an example. The cascade control leads to a substantially better control behavior than the single loop control.

1. INTRODUCTION

Unidirectional converters in their basic configuration are characterized by an asymmetrical structure regarding their topology and/or regarding their controllability. Switching instants and conduction intervals of the diodes on the secondary are - dependent on the converter topology (buck or boost converters etc.) - determined indirectly by changing the switching status of the power transistor on the primary.

An intrinsic limitation of this concept is given by the direction of current and energy flow (first quadrant of the current-voltage phase plane) which is determined by the direction of the electric valves.

Bidirectional power flow between constant voltage (current) sources requires replacement of the unidirectional power semiconductor devices by an antiparallel combination of a directly (power transistor) and an indirectly (diode) controllable electrical valve. This results in a unidirectionally controllable power semiconductor. However, this requires fixed voltage polarity,

equivalent to restriction to the first and second quadrants of the current-voltage plane.

The application of this general concept to a buck-boost converter structure leads to a topology with a remarkably simple topology. For further details of the converter structure see [1].

The stationary system condition is characterized by a time constant average energy content of the primary and secondary electrical and magnetic energy storage devices. This equilibrium between energy input and output corresponds to a duty ratio defined only by the voltage ratios (and turns ratios) of primary and secondary independent of the energy flow direction. This is shown in [1,2]. Idealized components are assumed and the push-pull control of transistors T_1 and T_2 is applied as indicated in Fig.1.

Vice versa by giving a duty ratio (for stationary, i.e. equilibrium operation) the voltage ratio of the converter can be varied to a large extent.

Continuous operation is given if the transistor on the primary is turned on again before i_{d2} reaches zero.

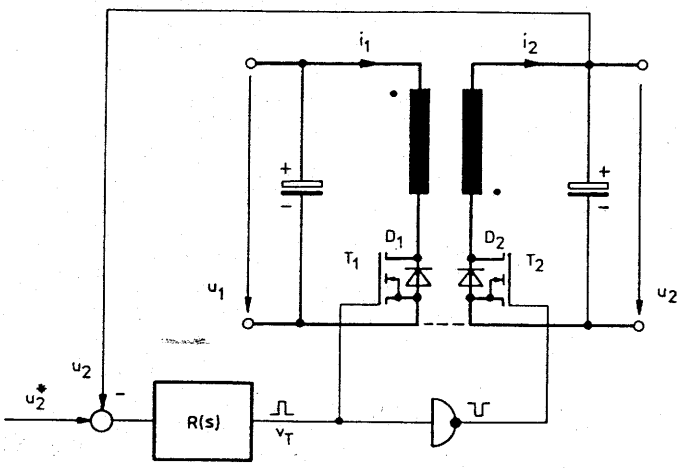

Fig.1 Bidirectional converter with push-pull control (basic structure)

2. MODEL REPRESENTATION OF THE BIDIRECTIONAL CONVERTER

For the derivation of the model equations for the bidirectional converter compare [1].

Parasitic elements considered are the (ohmic) resistances on the primary and secondary R_1, R_2 (consisting of the sums of the wind-

ing resistances and the R_{DSon} of the semiconductor switches). The duty ratio shall be defined as

$$\alpha = V_T = \frac{t_{on}}{T} \quad . \tag{1}$$

Weighed by this duty ratio, the combination of the two sets of equations for the two switching intervals (t_{on} and t_{off} of T_1) of the converter yields

$$\frac{d(u_c)}{dt} = - \frac{u_c}{C \cdot R} + (1-\alpha) \cdot \frac{N_1}{C \cdot N_2} \cdot i_1 \quad , \tag{2}$$

$$\frac{d(i_1)}{dt} = - (1-\alpha) \cdot \frac{N_2}{N_1} \cdot \frac{u_c}{L_2} - i_1 \cdot \left[\frac{R_1}{L_1} \cdot \alpha + (\alpha-1) \cdot \frac{R_2}{L_2} \right] + \alpha \cdot \frac{u_1}{N_1} \quad . \tag{3}$$

This set of equations is transformed into a linearized system around the operating point by introducing

$$\begin{aligned} u_c &= U_{co} + \hat{u}_c \quad , \\ i_1 &= I_{1o} + \hat{i}_1 \quad , \\ \alpha &= \alpha_o + \hat{\alpha} \quad , \end{aligned} \tag{4}$$

$$\begin{bmatrix} \frac{d(\hat{u}_c)}{dt} \\ \frac{d(\hat{i}_1)}{dt} \end{bmatrix} = \begin{bmatrix} A_{11} & A_{12} \\ A_{21} & A_{22} \end{bmatrix} \cdot \begin{bmatrix} \hat{u}_c \\ \hat{i}_1 \end{bmatrix} + \begin{bmatrix} B_{11} \\ B_{21} \end{bmatrix} \cdot \hat{\alpha} \tag{5}$$

with

$$A_{11} = - \frac{1}{R_o \cdot C} \quad , \qquad A_{12} = (1-\alpha_o) \cdot \frac{N_1}{C \cdot N_2} \quad ,$$

$$A_{21} = - \frac{1-\alpha_o}{L_2} \cdot \frac{N_2}{N_1} \quad , \quad A_{22} = - \left[\alpha_o \cdot \frac{R_1}{L_1} + (1-\alpha_o) \cdot \frac{R_2}{L_2} \right] , \tag{6}$$

$$B_{11} = - \frac{I_{1o} \cdot N_1}{C \cdot N_2} \quad , \quad B_{21} = \frac{U_{1o}}{L_1} + \frac{U_{co} \cdot N_2}{L_2 \cdot N_1} + \left[\frac{R_2}{L_2} - \frac{R_1}{L_1} \right] \cdot I_{1o} \cdot$$

This leads to the following structure diagram (Fig.2).

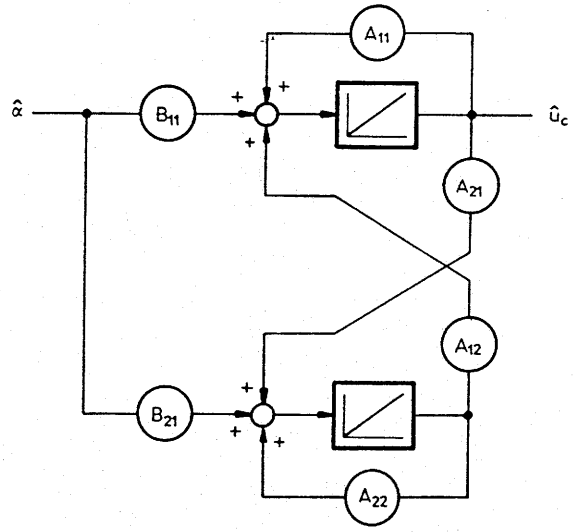

Fig.2 Structure diagram of the linearized bidirectional push-pull converter

The relationship for the stationary case results from:

$$\frac{1}{C}\cdot\frac{N_1}{N_2}\cdot I_{1o}\cdot(1-\alpha) - \frac{U_{co}}{R\cdot C} = 0 \qquad (7)$$

$$\frac{R_2}{L_2}\cdot(\alpha-1)\cdot I_{1o} + \frac{N_2}{N_1\cdot L_2}\cdot(\alpha_o-1)\cdot U_{co} + (U_{1o}+R_1\cdot\alpha_o)\cdot\frac{I_{1o}}{L_1} \qquad (8)$$

In the operating point (given by U_{1o}, U_{co}, I_{1o} and α_o) we can calculate from Eq.(5) the transfer function between output voltage u_c and the duty ratio α.

We receive $$u_c(s) = G_{u\alpha}(s)\cdot\alpha(s) \qquad (9)$$

with $$G_{u\alpha}(s) = \frac{s\cdot B_{11} + A_{12}\cdot B_{21} - A_{22}\cdot B_{11}}{s^2 - s\cdot(A_{11}+A_{22}) + \det A} \qquad (10)$$

3. THE BIDIRECTIONAL CONVERTER WITH CASCAD CONTROL

By linearization in the operating point the system of nonlinear equations (Eqs. 2,3) has been transformed into a linear one (Eq.5). Therefore it has been possible to give a transfer function of the bidirectional converter (Eq.10). Now it is possible

to use the means of controller dimensioning for linear systems. One has to keep in mind, however, that the controller based on the dimensioning really works as designed only in the chosen operating point.

The research in [2] has shown that the control quality of a single loop voltage control cannot meet higher standards. Damping of the system basically is given by the load. Stability considerations have shown very unfavorable positions of the system poles and zeros. The controller such dimensioned is only applicable for a limited operating region.

3.1 Partial transfer functions

Dividing the overall transfer function into two partial transfer functions ($G(s)=G_{i\alpha}(s)\cdot G_{ui}(s)$) makes it possible to design a two loop control stucture. Thereby $G_{i\alpha}(s)$ represents the relationship of the duty ratio and the converter current and $G_{ui}(s)$ gives the relationship between converter current and output voltage.

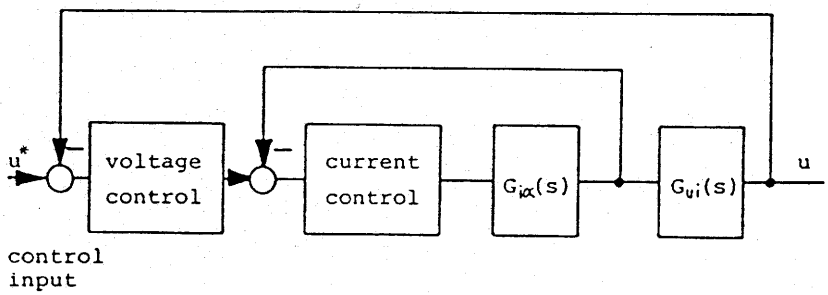

Fig.3 Cascade control structure

From a state vector representation

$$\begin{aligned} x &= A\cdot x + B\cdot u \\ y &= C\cdot x + D\cdot u \end{aligned} \qquad (11)$$

we can (according to [4,p.300]) determine the transfer function as

$$G(s) = c^T\cdot(s\cdot I - A)^{-1}\cdot b + d \qquad (12)$$

For the determination of the transfer function $G_{i\alpha}$ (which gives the relationship between converter current i_1 and the duty ratio α, we have $c^T=(0,1)$ and $d=0$. This results in

$$G_{i\alpha}(s) = \frac{s\cdot B_{21} + A_{21}\cdot B_{11} - A_{22}\cdot B_{11}}{s^2\cdot B_{21} + A_{21}\cdot B_{11} - A_{11}\cdot B_{21}} \qquad (13)$$

The relationship between output voltage u_c and converter current i_1 is given by

$$G_{ui}(s) = \frac{s \cdot B_{11} + A_{12} \cdot B_{21} - A_{22} \cdot B_{11}}{s \cdot B_{21} + A_{21} \cdot B_{11} - A_{11} \cdot B_{21}} \quad . \tag{14}$$

The overall transfer function of the converter system now is split into two partial transfer functions. Now one can design a controller for the current control section and thereby stabilize the inner loop. The transfer function resulting from this now together with the relationship between converter current and output voltage $G_{ui}(s)$ (Eq.14) represents the section to be controlled for the voltage control. The voltage controller now can be designed seperately. For the design we can apply now all means for the control design for linear systems (see, e.g., [4]). For the application of cascade control for conventional SMPS there exist numerous references (e.g., [5-7]).

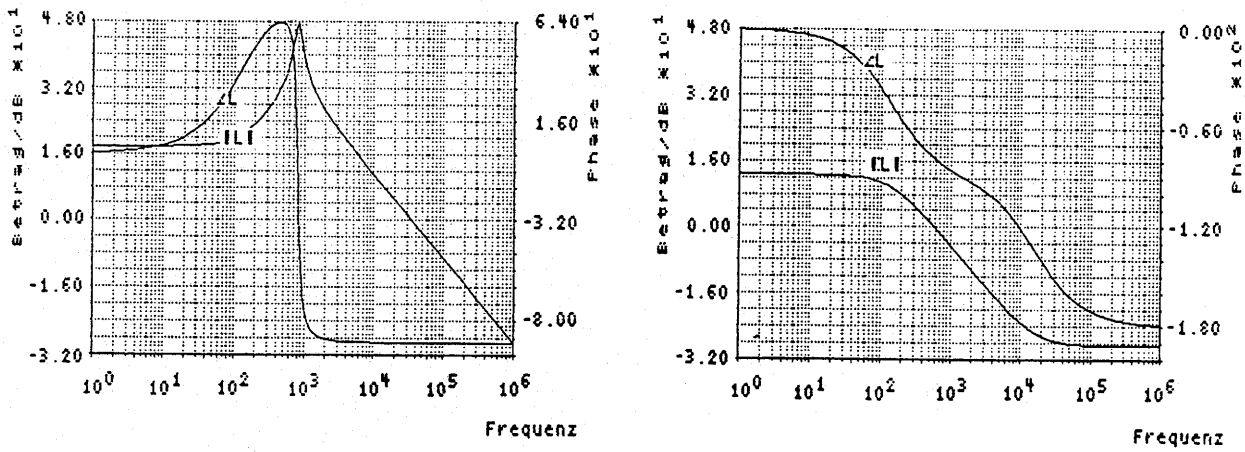

a) $G_{i\alpha}(s)$ b) G_{ui}

Fig.4 Bode diagrams for the partial transfer functions

3.2 Inner Contol Loop - Inner Loop Current Controller

3.2.1 Design of the P (Proportional) Controller

The transfer function of the current control loop results in

$$G_{iP}(s) = K_P \cdot \frac{B_{21} \cdot s + A_{21} \cdot B_{11} - A_{11} \cdot B_{21}}{s^2 + s \cdot (-A_{11} - A_{22} + K_P \cdot B_{21}) + detA + K_P \cdot bc} \tag{15}$$

with $detA = A_{11} \cdot A_{22} - A_{21} \cdot A_{12}$

$ab = A_{21} \cdot B_{11} - A_{11} \cdot B_{21}$ (see Eq.19) (16)

$bc = A_{12} \cdot B_{21} - A_{22} \cdot B_{11}$

3.2.2 Design of the PI (Proportional-Integral) Controller

The transfer function of the controller is

$$G_{iR}(s) = \frac{K_R \cdot (1+s \cdot T_R)}{s \cdot T_R} \quad ; \tag{17}$$

Therefore we receive for the current control with a PI controller

$$G_{iPR}(s) = \frac{s^2 \cdot r_1 + s \cdot r_2 + r_3}{s^3 \cdot t_1 + s^2 \cdot t_2 + s \cdot t_3 + t_4} \quad . \tag{18}$$

For abbreviation we set

$$\begin{aligned} r_1 &= K_R \cdot B_{21} \cdot T_R \\ r_2 &= K_R \cdot (B_{21} + T_R \cdot ab) \\ r_3 &= K_R \cdot ab \\ t_1 &= T_R \\ t_2 &= T_R \cdot (K_R \cdot B_{21} - A_{11} - A_{22}) \\ t_3 &= detA \cdot T_R + K_R \cdot T_R \cdot ab + K_R \cdot B_{21} \end{aligned} \tag{19}$$

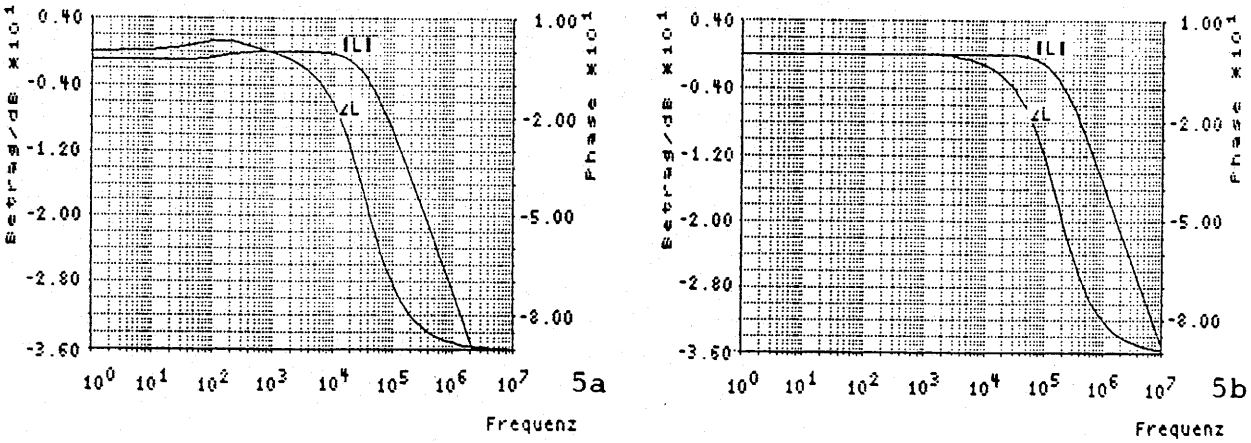

Fig.5 Bode diagrams for the closed current control loop for a) P-controller, b) PI-controller

3.3 The Outer Control Loop - the Voltage Control

In a second step now an outer loop voltage control will be designed. Dependent on the current control realization we receive different systems to be controlled for the voltage controller.

3.3.1 Controlled System for Voltage Control with Inner Loop P Current Control Circuit

$$G_u(s) = K_P \cdot \frac{B_{11} \cdot s + A_{12} \cdot B_{21} - A_{22} \cdot B_{11}}{s^2 + s \cdot (-A_{11} - A_{22} + K_P \cdot B_{21}) + detA + K_P \cdot ab} \tag{20}$$

3.3.2 Controlled System for Voltage Control with Inner Loop PI Current Control Circuit

$$G_u(s) = \frac{\beta_3 \cdot s^3 + \beta_2 \cdot s^2 + \beta_1 \cdot s + \beta_0}{\delta_4 \cdot s^4 + \delta_3 \cdot s^3 + \delta_2 \cdot s^2 + \delta_1 \cdot s + \delta_0} \quad . \qquad (21)$$

For abbreviation we set

$$\begin{aligned} \beta_3 &= r_1 \cdot B_{11} \\ \beta_2 &= r_2 \cdot B_{11} + r_1 \cdot bc \\ \beta_1 &= r_3 \cdot B_{11} + r_2 \cdot bc \\ \beta_0 &= bc \cdot r_3 \\ \delta_4 &= t_1 \cdot B_{21} \\ \delta_3 &= t_2 \cdot B_{21} + t_1 \cdot ab \\ \delta_2 &= t_3 \cdot B_{21} + t_2 \cdot ab \\ \delta_1 &= t_4 \cdot B_{21} + t_3 \cdot ab \\ \delta_0 &= t_4 \cdot ab \end{aligned} \qquad (22)$$

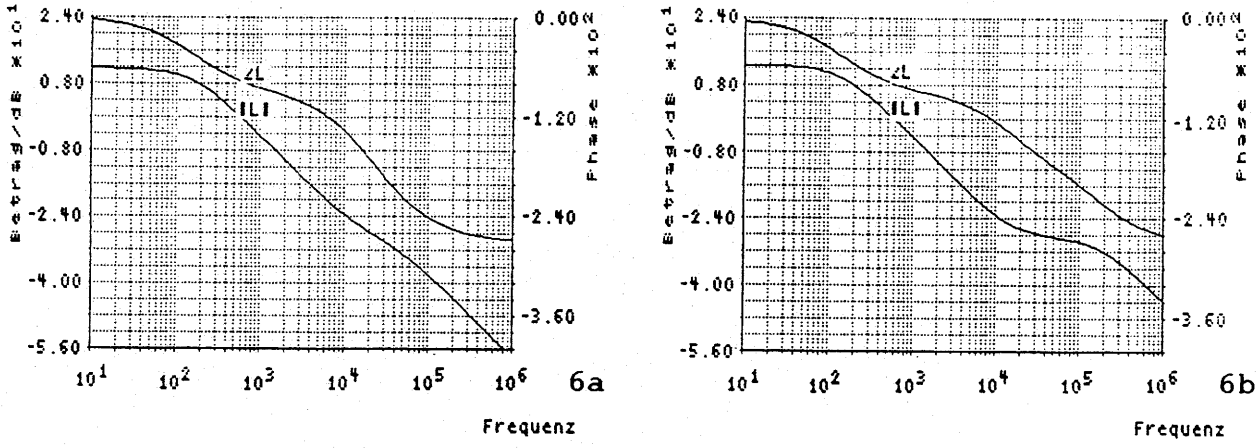

Fig.6 Bode diagrams for the open voltage control loop with a) P-current-controller, b) PI-current-controller

3.3.3 Voltage Controller

The transfer functions for a

P-controller is $G_{uP}(s) = K_{Pu}$ (23)

and for a PI-controller $G_{uPI}(s) = \frac{K_{Iu} \cdot (1 + s \cdot T_{Iu})}{s \cdot T_{Iu}}$ (24)

3.4 Transfer Function for the Overall System

For the overall system the following transfer functions result

3.4.1 P-voltage-controller with P-current-controller

$$G(s) = \frac{\sigma_1 \cdot s + \sigma_0}{s^2 + \tau_1 \cdot s + \tau_0} \tag{25}$$

with
$$\begin{aligned} \sigma_1 &= K_{Pu} \cdot K_{Pi} \cdot B_{11} \\ \sigma_0 &= K_{Pu} \cdot K_{Pi} \cdot bc \\ \tau_1 &= -A_{11} - A_{22} + K_{PiP} \cdot B_{21} + K_{Pu} \cdot K_{Pi} \cdot B_{11} \\ \tau_0 &= \det A + K_{Pi} \cdot ab + K_{Pu} \cdot K_{Pi} \cdot bc \end{aligned} \tag{26}$$

3.4.2 PI-voltage-controller with P-current-controller

$$G(s) = \frac{\delta_2 \cdot s^2 + \delta_1 \cdot s + \delta_0}{\mu_3 \cdot s^3 + \mu_2 \cdot s^2 + \mu_1 \cdot s + \mu_0} \tag{27}$$

with
$$\begin{aligned} \delta_2 &= K_{Iu} \cdot K_{Ii} \cdot B_{11} \cdot T_{Iu} \\ \delta_1 &= K_{Iu} \cdot K_{Ii} \cdot (B_{11} + T_{Iu} \cdot bc) \\ \delta_0 &= K_{Iu} \cdot K_{Ii} \cdot bc \\ \mu_3 &= T_{Iu} \\ \mu_2 &= T_{Iu} \cdot (-A_{11} - A_{22} + K_P \cdot B_{21}) + K_{Iu} \cdot K_{Ii} \cdot B_{11} \cdot T_{Iu} \\ \mu_1 &= T_{Iu} \cdot (\det A + K_P \cdot ab) + K_{Iu} \cdot K_{Ii} \cdot (B_{11} + T_{Iu} \cdot bc) \\ \mu_0 &= K_{Iu} \cdot K_{Ii} \cdot bc \end{aligned} \tag{28}$$

3.4.3 PI-voltage-controller with PI-current-controller

$$G(s) = \frac{\Phi_4 + \Phi_3 + \Phi_2 \cdot s^2 + \Phi_1 \cdot s + \Phi_0}{\Omega_5 \cdot s^5 + \Omega_4 \cdot s^4 + \Omega_3 \cdot s^3 + \Omega_2 \cdot s^2 + \Omega_1 \cdot s + \Omega_0} \tag{29}$$

with
$$\begin{aligned} \Phi_4 &= T_{Iu} \cdot r_1 \cdot B_{11} \\ \Phi_3 &= T_{Iu} \cdot r_2 \cdot B_{11} + r_1 \cdot B_{11} + T_{Iu} \cdot r_1 \cdot bc \\ \Phi_2 &= T_{Iu} \cdot r_3 \cdot B_{11} + r_2 \cdot B_{11} + T_{Iu} \cdot r_2 \cdot bc + r_1 \cdot bc \\ \Phi_1 &= r_3 \cdot B_{11} + r_3 \cdot B_{11} + T_{Iu} \cdot r_3 \cdot bc \\ \Phi_0 &= r_3 \cdot bc \\ \Omega_5 &= t_1 \cdot B_{21} \\ \Omega_4 &= t_2 \cdot B_{21} + t_1 \cdot ab + \Phi_4 \\ \Omega_3 &= t_3 \cdot B_{21} + t_2 \cdot ab + \Phi_3 \\ \Omega_2 &= t_4 \cdot B_{21} + t_3 \cdot ab + \Phi_2 \\ \Omega_1 &= t_4 \cdot ab + \Phi_1 \\ \Omega_0 &= \Phi_0 \end{aligned} \tag{30}$$

The controller design was performed with the means of the classical linear control theory. For the practical design we have to consider the limitations of the duty ratio and of maximum permissible transformer (converter) current, however. The controller

parameters therefore have to be checked for their validity. This is possible by using the model according to Eqs.(2,3).

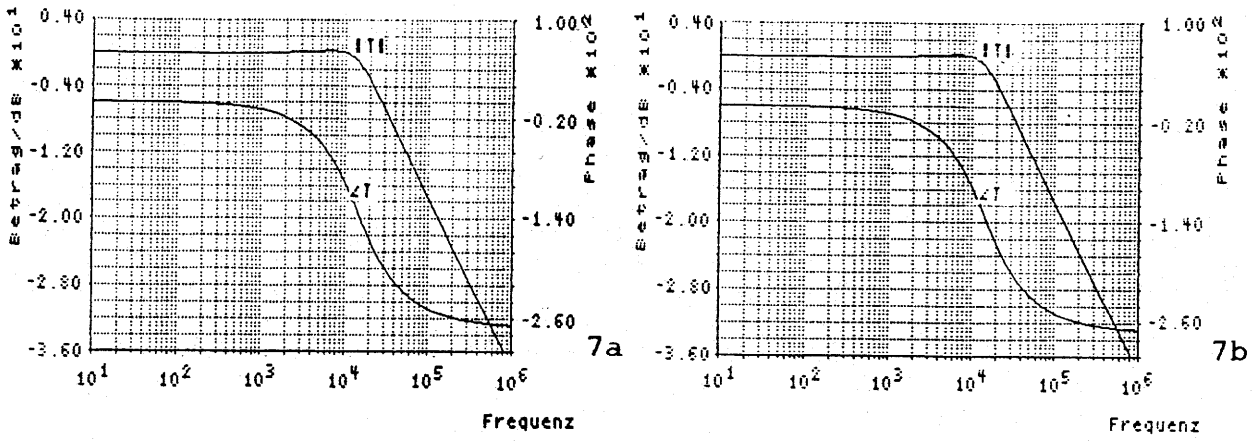

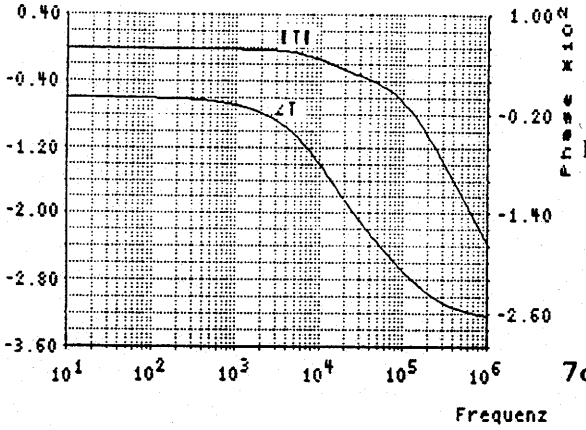

Fig.7 Bode diagrams of the closed system
a) P-voltage and P-current contoller
b) PI-voltage and P-current controller
c) PI-voltage and PI-current controller

3.5 System step response

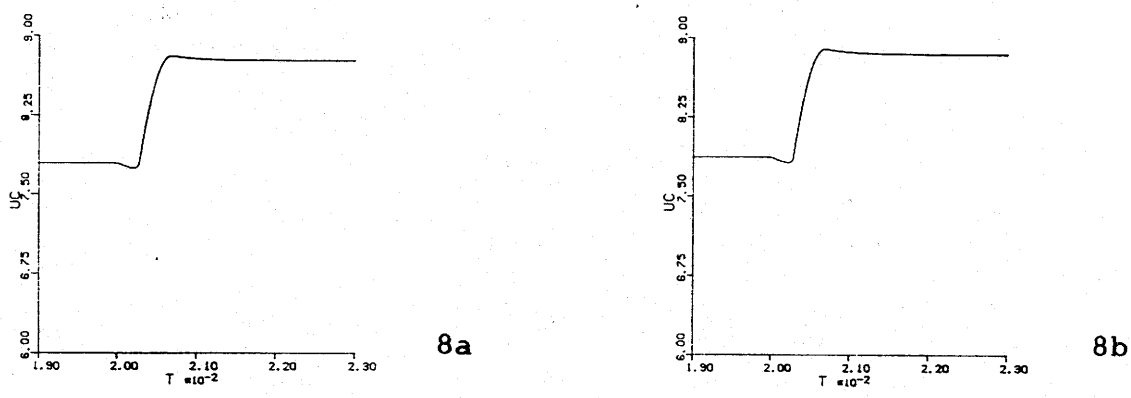

Fig.8 a) Closed loop response for the P-P-structure
b) Closed loop response for the PI-P-structure

Fig.8 shows the closed loop step responses calculated based on the nonlinear model (Eq.2,3) for a P-voltage-controller with P-current-controller (a) and for a PI-voltage-controller with a P-current-controller (b). With the PI-PI structure the performance cannot be increased significally.

4. Conclusions

The two loop control structure consists of an inner current control loop and an outer voltage control loop. The research has shown that this results in a substantially better control behavior because it is possible to stabilize the two loops then very efficiently.

Starting with the structure diagram and the transfer function derived in [2] the partial transfer functions are calculated. The system behavior of the system sections has been analyzed and a dimensioning of the two controller sections has been performed. Selected bode diagrams for different controllers are investigated. Finally the controller design has been shown for an example.

REFERENCES

[1] Kolar,J.W.,Himmelstoss,F.A.,and Zach,F.C.: " Analysis of the Control Behavior of a Bidirectional High-Frequency DC-DC-Converter", PCIM 88,Munich May 8-10,1988,pp.344-359

[2] Himmelstoss, F.A., Kolar,J.W., and Zach,F.C.: " Analysis of closed-loop control behavior of a bidirectional high frequency DC-DC converter", PCIM 88,Tokio Dec 8-10,1988,pp.174-184

[3] Middlebrook,R.D.,Cuk,S.:"Advances in Switched-Mode Power Con-Conversion", Vol.1,Pasadena:Teslaco.1981

[4] Föllinger,O.:"Regelungstechnik",Heidelberg:Hüthig Verlag.1984

[5] Mitchell,D.M.: "An Analytical Investigation of Current-Injected Control for Constant-Frequency Switching Regulators", IEEE Trans. PE, Vol.1, No.3, pp.167-174

[6] Sato,T.,Nakano T.,Harada K.:"The Overload-Protection Characteristics of the Current-Mode DC-to-DC Converter; Analysis and Improvement", PESC '88 RECORD, pp.830-835

[7] Kawabata T., Shikano Y., Higashino S., Yamamoto Y., Udaka M., Kawagishi K.: "Chargerless UPS Using Multi-functional BIMOS Inverter - Sinusoidal voltage waveform inverter with current minor loop, IEEE IAS Annual Meeting 1986, pp.513-520